2.3 NUMERICAL SIMULATION OF A CONVECTIVE TURBULENCE ENCOUNTER

Fred H. Proctor and David W. Hamilton
NASA Langley Research Center, Hampton, Virginia
and
Roland L. Bowles
AeroTech Research, Inc., Hampton, Virginia

1. INTRODUCTION

A major portion of the accidents from aircraft turbulence encounters are within close proximity of atmospheric convection (Kaplan et al. 1999). The National Aeronautics and Space Administration (NASA), through its Aviation Safety Program, is testing technologies that will reduce the risk of injuries from these types of encounters. Primary focus of the Turbulence Prediction And Warning Systems (TPAWS) element within this program is the characterization of turbulence and its environment, and the development and testing of hazard-estimation algorithms for both radar and *in situ* detection. The ultimate goal is to operationally test onboard sensors that will provide ample warning prior to encounters with hazardous turbulence. In support of turbulence characterization, numerical modeling of atmospheric convection is being conducted using a large eddy simulation model. A special need for the modeling is to provide realistic data sets for developing and testing turbulence detection sensors.

During two test days in December 2000, regions of convective turbulence were purposefully encountered by NASA Langley's *B-757* (see Hamilton and Proctor 2002a, 2002b). Regions with moderate or greater radar reflectivity, i.e. *RRF* > 35 *dBZ*, were avoided as routinely done by commercial air carriers. Turbulence measurements from the *in situ* system were quantified in terms of root-mean-square (RMS) normal loads (σ_{ng}), where $0.20\ g \le \sigma_{ng} \le 0.30\ g$ is considered moderate and $\sigma_{ng} > 0.30\ g$ is severe (Pantley 1989). The turbulence event selected for our study was the strongest event encountered during the fall-2000 flight tests. This event, 191-6 (referred as 191.3 in Hamilton and Proctor 2002a, 2002b), had a peak turbulence intensity of $\sigma_{ng} = 0.44\ g$. This event was encountered northeast of Tallahassee (TLH), just north of the Florida-Georgia boarder on 14 December 2000 (Fig. 1). The turbulence was characterized by sharp oscillations in vertical velocity over a distance of ~5 *km*, as NASA Langley's B-757 penetrated updraft plumes near the top of a narrow line of thunderstorms. At the time of penetration, the aircraft was at an altitude of 10.3 *km* above ground level (AGL) and had an air speed of about 235 *m/s*.

Data from onboard Doppler radar, *in situ* wind and temperature measurements, and recorded NEXRAD radar data are available for comparison with the numerical simulation of this case. This paper will describe results from the simulation of this event. The conditions associated with the actual turbulence encounter are described in Hamilton and Proctor (2002a, 2002b).

2. THE MODEL AND INITIAL CONDITIONS

The numerical simulation is carried out with the Terminal Area Simulation System (TASS), which is a large eddy simulation model developed for simulating convective clouds and atmospheric turbulence (Proctor 1987, Proctor et al. 2002).

Corresponding author address: Fred H. Proctor, NASA Langley Research Center, MS 156A, Hampton, VA, 23681-2199; email: f.h.proctor@larc.nasa.gov.

Figure 1 . *Orientation of TASS domain relative to convective line. Observed composite radar reflectivity field and flight path depicted near the time of event 191-6. Florida border depicted by heavy line.*

The simulation is initialized with a vertical distribution of temperature, dew point, and wind velocity, representative of the environment near the time and location of the turbulence event. Since observed profiles were unavailable at this time and location, a forecast sounding was used from a real-time mesoscale model (Kaplan et al. 2002).

The model domain is rotated 66° clockwise such that the *x*-coordinate is orthogonal to the convective line and the *y*-coordinate is parallel to the line (see Fig. 1). The physical size of the domain is 25 *x* 25 *x* 14 *km*. The grid size is uniform at 100 *m* over most of the domain, except below an altitude of 2000 *m* where grid stretching shrinks the vertical size to 50 *m*. The domain is resolved by 148 vertical levels, with each horizontal plane having 251 *x* 251 grid points.

In order to model scales of motion important for aircraft response, high resolution is needed. Results from a frequency-domain flight dynamics model (Bowles 1999, 2000) indicates that scales of motion as small as 50 *m* (wave number of 0.126 *rad/m*) are needed in order to capture at least 97% of the cumulative aircraft load distribution (Fig. 2). Available computer capability and the size of the computations restricts the grid size to about 100 *m*. Although this resolution misses scales that are important for aircraft response, the model's ability to simulate the larger-scale features of a convective-turbulence event can be assessed. This evaluation is discussed in the first part of the next section. High-resolution turbulence fields are achieved by extracting a subdomain from the numerical simulation and merging it with subgrid turbulence

fields. Results from this procedure are discussed in the second part of the next section.

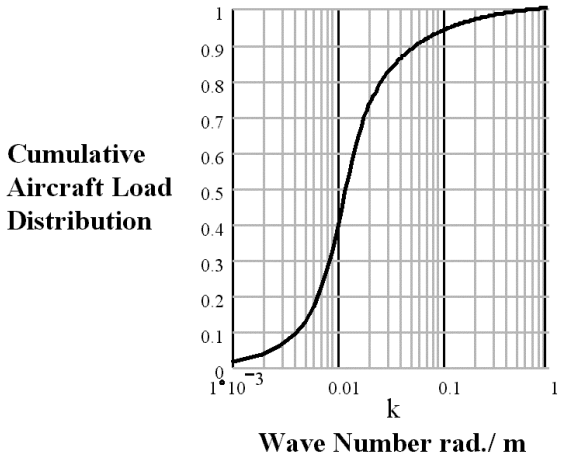

Figure 2. *Cumulative distribution of normalized aircraft loads as a function of wave number. Aircraft calculation based on B-757-200 frequency domain model. Assumes von Karman turbulence spectrum with an outer scale of 300 m and σ_w=1 m/s.*

3. Results

Results from the TASS 100*m* simulation have been compared with observations derived from ground based NEXRAD radar and *B-757* flight data (see Proctor et al. 2002). Table 1 shows comparisons between simulation and observations of selected features. Orientation and width of the convective line, storm top, radar reflectivity, and cell movement all tend to agree with observed values.

TABLE 1. MODEL COMPARISON.

Variable	TASS	Observed
Orientation of Line	*WSW-ENE*	*WSW-ENE*
Peak Storm Tops	11.5 *km*	11.8 *km*
Peak Radar Reflectivity at Ground	53.5 *dBZ*	55 *dBZ*
Peak Radar Reflectivity at *z*=9 *km*	38.9 *dBZ*	40 *dBZ*
Cell Motion (toward)	*ENE* at 19 *m/s*	*ENE* at 17 *m/s*
Width of Convective Line near Ground Level (based on 20 *dBZ*)	6 *km*	8 *km*
Peak Eddy Dissipation Rate ($m^{2/3}$ s^{-1})	0.86	0.74
Horizontal Scale of Turbulence Patch at Flight Level	5 *km*	5-6 *km*

A three-dimensional perspective of the simulated convective line appears quite realistic, exhibiting cumulus turrets, anvil outflow, and overshooting tops (Fig. 3). The convective cells exhibit downwind tilt (toward the northeast) with most of the anvil outflow spreading in that direction. During the actual encounter, the NASA *B-757* flew toward the northeast parallel to the line and entered the overshooting cloud areas near the storm tops. Severe turbulence was encountered as the aircraft skirted the northwestern flank of the convective line.

The radar reflectivity from the onboard radar just before encountering event 191-6 is shown in Fig. 4. A simulation of this radar using the TASS data set is shown for comparison in Fig. 5. Both show similar scale and intensity, although details in the echo structure differ.

An energy spectra computed from the TASS velocity data at flight altitude are shown in (Fig. 6). The spectra appear to have an inertial subrange with a -5/3 slope especially at larger wavelengths. At smaller wavelengths, however, the spectra show a steeper slope than the theoretical -5/3 slope. This drop-off in energy at higher wavenumbers is often found in other LES studies (e.g., Schmidt and Schumann 1989), and is theoretically expected since values at each grid cell represent volumetric averages rather than point values (Moeng and Wyngaard 1988).

3.1 Merging with Subgrid Turbulence

Although the 100*m* TASS simulation was able to simulate the larger-scale features of the turbulence event, it could not resolve the smaller-scales of motion important for aircraft response calculations. Figure 6 shows that only wavelengths greater than 600 *m* (6 grid points) are adequately resolved, and according to Fig. 2 only 40% of the cumulative aircraft load is captured at these frequencies. Since finer resolution is needed for proper aircraft response simulation, high-resolution subgrid turbulence fields were merged with a subdomain of the TASS simulation. This data set was generated by NCAR using the following procedure (Sharman 2001):

1) A sub-volume of the domain was selected which encompassed the turbulence event.
2) The variables were interpolated to a 25 *m* grid, within a 12.8 *km x* 12.8 *km* horizontal and 3.2 *km* vertical subdomain.
3) Following a technique devised by Frehlich et al. (2001), subgrid wind fields using a von Karman algorithm were then merged with the TASS data. The von Karman subgrid parameters (variance and outer length scale) were determined from a best fit of the model generated structure functions (after interpolation) to the desired Kolmogorov behavior.

Subgrid fields are only added to the velocity fields. Other fields, such as radar reflectivity are simply interpolated to the higher-resolution subdomain.

3.2 Hazard Analysis

Aircraft response to turbulence flow is most affected by along-track gradients in vertical velocity. Aircraft response can be deduced from flight-dynamic models for a single path (Bowles 1999, 2000). A more general algorithm that can be applied to large, multi-dimensional data sets is proposed below and is applied to the merged data set for case 191-6. For a particular aircraft, the RMS normal load can be estimated from σ_w using look-up tables (Bowles 2000); i.e.

$$\sigma_{ng}(x,y) = Func\{\sigma_w, \textit{altitude, aircraft type, weight, airspeed}\}$$

The σ_w fields can be computed for any horizontal plane in the merged data set, by using a moving average as:

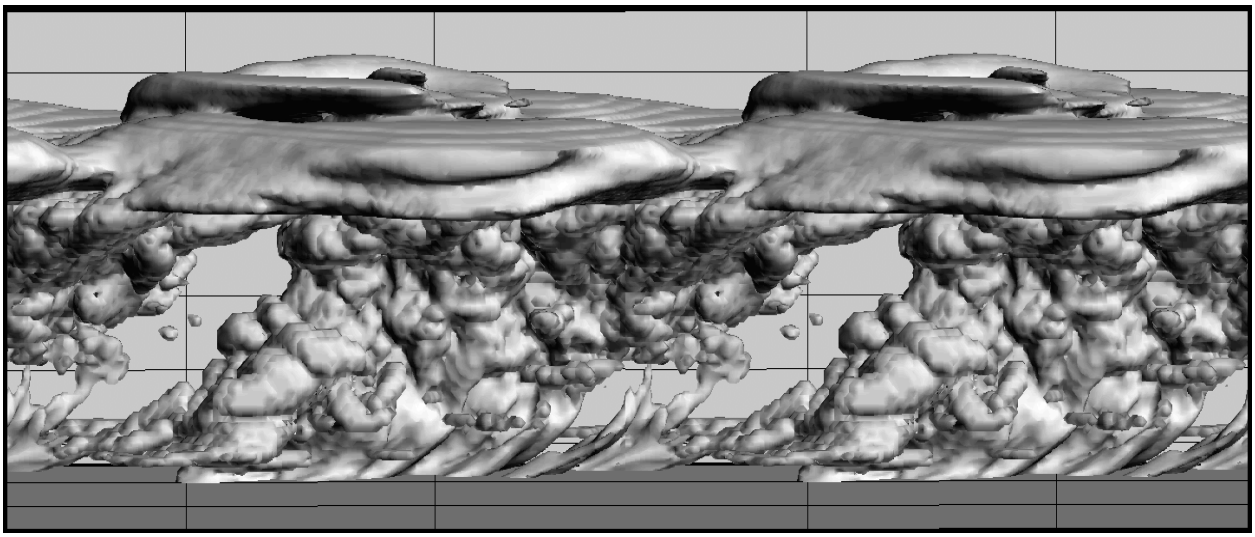

Figure 3. *TASS generated convective-cloud line for event 191-6 as viewed from southeast.*

.

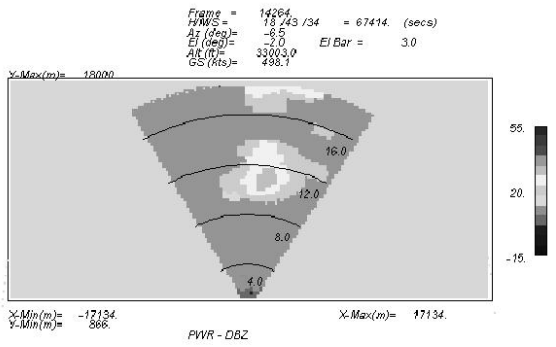

Figure 4. *Radar reflectivity (dBZ) from onboard turbulence radar. Observed just prior to encounter with event 191-6. Range rings every 4 km.*

$$\sigma_w(x,y)=\left[\frac{1}{L_xL_y}\int_{x-\frac{L_x}{2}}^{x+\frac{L_x}{2}}\int_{y-\frac{L_y}{2}}^{y+\frac{L_y}{2}}\{w(x',y')-\overline{w}(x,y)\}^2\,dx'dy'\right]^{\frac{1}{2}}$$

where the averaging interval along the *x* and *y* coordinates is L_x, L_y, respectively. The average vertical wind, $\overline{w}$, is computed from the vertical wind, *w*, as:

$$\overline{w}(x,y)=\frac{1}{L_xL_y}\int_{x-\frac{L_x}{2}}^{x+\frac{L_x}{2}}\int_{y-\frac{L_y}{2}}^{y+\frac{L_y}{2}}w(x',y')dx'dy'$$

The value for the averaging interval, L_x=L_y = 1000 *m*, is chosen to correspond to an ~5 *s* averaging period for a commercial jet at cruise speeds. Hence, the second moment of the *w*-field is computed assuming a 1 *x* 1 *km* moving box.

The RMS normal load (σ_{ng}) is computed from the σ_w fields, assuming aircraft parameters for NASA's *B-757*. Since calculations are independent of aircraft heading, evaluation of the turbulence field is relatively simple. Regions with $\sigma_{ng} > 0.3$ *g* represent severe turbulence, while $0.20\ g \le \sigma_{ng} \le 0.30\ g$ represent moderate turbulence. Comparison between the σ_{ng} and radar reflectivity fields of the merged data set is shown in Figs. 7 and 8. Note that moderate intensity of turbulence is

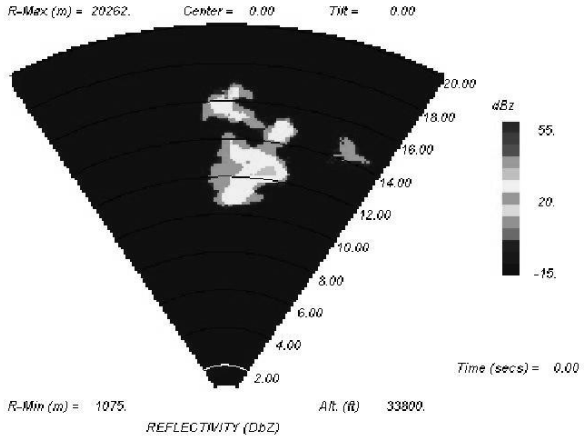

Figure 5. *Radar reflectivity (dBZ) from simulation of onboard radar using TASS data set. Simulation assumes same altitude and heading as in Fig. 4. Range rings every 2 km.*

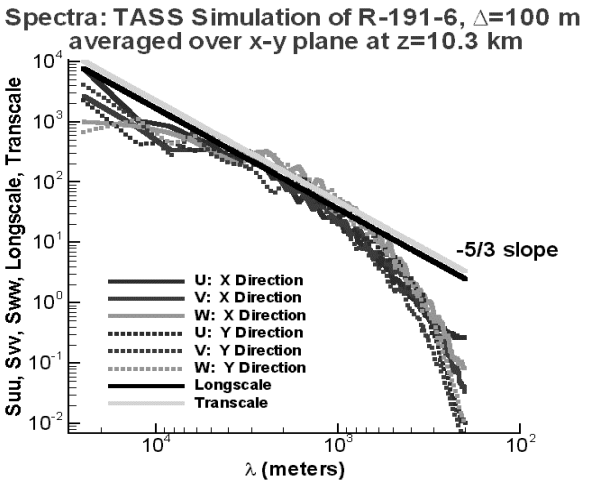

Figure 6. *Energy spectra from TASS, as computed from velocity field within 25x25 km horizontal plain at flight elevation.*

sometimes found in regions of weak radar reflectivity. The peak value of σ_{ng} of 0.37 *g* is associated with RRF less than 35 *dBZ*.

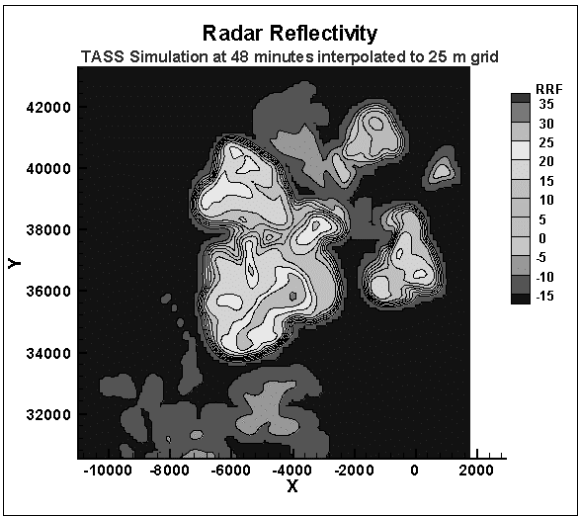

Figure 7. Horizontal cross-section of *TASS radar reflectivity field (dBZ) at flight level (z=10.3 km AGL).*

3.3 RMS Normal Load Comparison

Table 2 shows a comparison between peak RMS normal loads measured near the B-757 flight path with those simulated from the merged data set. All sources indicate a severe turbulence event whether from observed data or simulation.

TABLE 2. RMS NORMAL LOAD COMPARISON

Source	Peak σ_{ng} (*g's*)
In situ	0.44
Onboard Turbulence Radar^{+}	0.37
Ground-Based Doppler Radar^{+}	0.33
Flight Dynamics Simulation	0.36
Model Diagnostic from σ_w field	0.37
Radar Simulation with Model Data	0.33

$^{+}$*Computed from radar spectrum width*

4. Summary

A numerical simulation of a convective turbulence event is investigated and compared with observational data. The numerical results show severe turbulence of similar scale and intensity to that encountered during the test flight. This turbulence is associated with buoyant plumes that penetrate the upper-level thunderstorm outflow. The simulated radar reflectivity compares well with that obtained from the aircraft's onboard radar.

Resolved scales of motion as small as 50 *m* are needed in order to accurately diagnose aircraft normal load accelerations. Given this requirement, realistic turbulence fields may be created by merging subgrid-scales of turbulence to a convective-cloud simulation.

A hazard algorithm for use with model data sets is demonstrated. The algorithm diagnoses the RMS normal loads from second moments of the vertical velocity field and is independent of aircraft motion.

Acknowledgements

This research was sponsored by NASA's Aviation Safety Program. Numerical simulations were carried out on NASA supercomputers. Figures 4-5 were provided by Les Britt, RTI, under NASA contract NAS1-99074.

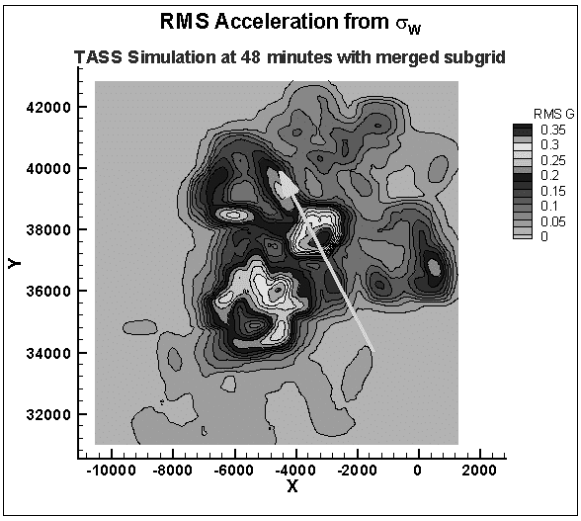

Figure 8. Same as Fig. 7, but t*urbulence hazard field (σ_{ng}).*

References

Bowles, R.L., 1999: Theoretical investigation of the relationship between airborne radar observables and turbulence induced aircraft g-loads. AeroTech Report ATR-12007, (prepared for NASA Langley Research Center).

-----, 2000: Aircraft centered hazard metric based on airborne radar turbulence observables. AeroTech Report ATR-12010, (prepared for NASA Langley Research Center).

Frehlich, R.G., L. Cornman, and R.Sharman, 2001: Simulation of three-dimensional turbulent velocity fields. J*. Applied Meteor*., **40**, 246-258.

Hamilton, D.W. and F.H. Proctor, 2002a: Meteorology associated with turbulence encounters during NASA's fall-2000 flight experiments. *40th Aerospace Sciences Meeting & Exhibit*, AIAA 2002-0943, 11pp.

-----,and -----,2002b: Convectively induced turbulence encountered during NASA's fall-2000 flight experiments. *10th Conference on Aviation, Range, and Aerospace Meteorology*, Portland OR, Amer. Meteor. Soc., paper 10.8.

Kaplan, M.L., Y-L. Lin, A.J. Riordan, K.T. Waight, K.M. Lux, and A.W. Huffman, 1999: Flight safety characterization studies, part I: turbulence categorization analyses. Interim Subcontrator Report to Research Triangle Institute, NASA contract NAS1-99074.

-----, J.J. Charney, K.T. Waight III, Y-L. Lin, K.M. Lux, A.W. Huffman, and J.D. Cetola, 2002: A real-time turbulence model (RTTM) designed for the operational prediction of aviation turbulence environments. *10th Conference on Aviation, Range, and Aerospace Meteorology*, Portland OR, Amer. Meteor. Soc.,paper 10.3.

Moeng, C. –H., and J.C. Wyngaard, 1988: Spectral analysis of large-eddy simulations of the convective boundary layer," *J. Atmos. Sci.*, **45**, 3573-3587.

Pantley, K. C., 1989: *Turbulence Near Thunderstorm Tops*. Master's Thesis, Department of Meteorology, San Jose State University, 132 pp.

Proctor F.H., 1987: The Terminal Area Simulation System, Volume 1: Theoretical Formulation. NASA Contractor Report 4046, DOT/FAA/PM-85/50, 1, 176 pp.

-----, D.W. Hamilton, and R.L. Bowles, 2002: Numerical study of a convective turbulence encounter. *40th Aerospace Sciences Meeting & Exhibit*, AIAA 2002-0944, 14pp.

Schmidt, H., and U. Schumann, 1989: Coherent structure of the convective boundary layer derived from large eddy simulations," *J. Fluid Mech.*, **200**, 212-248.

Sharman, R., 2001: 191-6 merged subgrid turbulence for t=48 min Deliverable to NASA from NCAR under NASA Contract.